Indolicidin Binding Induces Thinning of a Lipid Bilayer

Chris Neale,[†‡] Jenny C. Y. Hsu,[‡§] Christopher M. Yip,[‡§] and Régis Pomès[†‡*]
[†]Molecular Structure and Function, The Hospital for Sick Children, Toronto, Ontario, Canada; [‡]Department of Biochemistry and [§]Terrence Donnelly Centre for Cellular and Biomolecular Research, University of Toronto, Toronto, Ontario, Canada

ABSTRACT We use all-atom molecular dynamics simulations on a massive scale to compute the standard binding free energy of the 13-residue antimicrobial peptide indolicidin to a lipid bilayer. The analysis of statistical convergence reveals systematic sampling errors that correlate with reorganization of the bilayer on the microsecond timescale and persist throughout a total of 1.4 ms of sampling. Consistent with experimental observations, indolicidin induces membrane thinning, although the simulations significantly overestimate the lipophilicity of the peptide.

Received for publication 11 October 2013 and in final form 21 February 2014.

*Correspondence: pomes@sickkids.ca

Antimicrobial peptides are a component of the innate immune system of eukaryotes (1). As such, they must interact with pathogenic membranes, either during translocation or by disrupting their structural integrity (2). Here we examine the binding of the 13-residue cationic antimicrobial peptide indolicidin (3) (ILPWKWPWWPWRR-NH_2) to a lipid membrane as a first step towards elucidating its mechanism of action.

Molecular solutes interact with lipid membranes in many cellular processes (4). Computational approaches such as molecular dynamics simulations have been widely used to characterize these interactions (5). However, molecular dynamics simulations can require unfeasibly long times to reach equilibrium (6). Therefore, it is common to compute equilibrium properties of solute insertion into lipid bilayers using umbrella sampling (7) simulations in which the solute is restrained along the bilayer normal using harmonic restraining potentials, or umbrellas, centered at z_i^0 values distributed between bulk water and the bilayer center.

It is often assumed that equilibrium properties rapidly attain convergence in umbrella sampling simulations; accordingly, convergence measures are rarely published (8). However, we have recently shown that umbrella sampling simulations require up to 100 ns per umbrella (3 μs in total) to eliminate systematic sampling errors in the standard free energy of binding, ΔG^0_{bind}, of an arginine sidechain analog from bulk water to a lipid bilayer (8). The fact that umbrella sampling has been used to investigate the bilayer insertion of substantially larger solutes (9) motivates a systematic evaluation of statistical sampling convergence of ΔG^0_{bind} for indolicidin in a lipid bilayer.

To estimate ΔG^0_{bind} of indolicidin to a lipid bilayer, we conducted 60 sets of umbrella-sampling simulations while systematically varying the initial conformation. In each umbrella sampling simulation, each umbrella was simulated for 1.5 μs, yielding a total simulation time of 1.4 ms and 60 independent free energy or potential of mean force (PMF) profiles from bulk water to the center of a POPC (1-palmitoyl-2-oleoyl-*sn*-glycero-3-phosphatidylcholine) lipid bilayer.

The PMF profiles indicate that indolicidin strongly binds to the bilayer, partitioning inside the lipid headgroups (Fig. 1, *A* and *E*). Importantly, the mean estimate of ΔG^0_{bind} decays exponentially with equilibration time t_{eq}, indicating that systematic sampling errors in individual simulations continued to decrease throughout the 1.5-μs interval as rare events led to more favorable states (Fig. 1 *B*). The low frequency of transitions to more favorable states exacerbates the requirement for massive sampling using multiple independent simulations.

Computational limitations precluded extending all 60 sets of umbrella-sampling simulations to even longer times. Instead, we identified the two simulations at each umbrella that appeared to be most representative of equilibrium and extended each to 10 μs per umbrella (see Methods in the Supporting Material). The resulting estimates of ΔG^0_{bind} continued to decrease until $t_{\text{eq}} = 4$ μs (68 μs in total), after which they stabilized at the asymptotic limit of the exponential fit of the shorter simulation data ($\Delta G^0_{\text{bind}} = -26 \pm 5$ kcal/mol; Fig. 1 *C*).

As indolicidin approaches the bilayer, it is drawn closer (Fig. 2 *A*) as salt bridges form between the peptide and the phospholipid headgroups (Fig. 2 *B*), inducing their protrusion (Figs. 1 *D* and 2 *C*). At large separation distances, this state is attained only when the peptide becomes highly extended (Fig. 2, *D* and *E*). As indolicidin is inserted more deeply, the surface of the lipid bilayer invaginates (Figs. 1 *E* and 2 *C*), maintaining peptide-lipid salt bridges (Fig. 2 *B*) and leading to the formation of a pore when the solute is near the bilayer center (Figs. 1 *F* and 2 *C*, and see Fig. S2, Fig. S3, Fig. S4, and Fig. S5 in the Supporting

Editor: Scott Feller.
© 2014 by the Biophysical Society
http://dx.doi.org/10.1016/j.bpj.2014.02.031

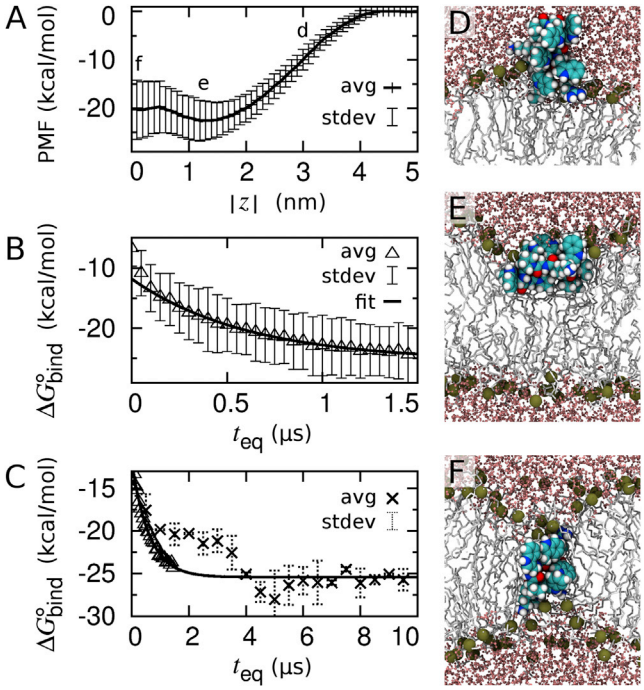

FIGURE 1 PMF for indolicidin partitioning into a POPC bilayer. (*A*) Average PMF from 60 independent umbrella-sampling simulations based on $1 < t \leq 1.5$ μs/umbrella. (*B*) Average ΔG^0_{bind} from 50-ns time intervals per umbrella ($t_{eq} < t \leq t_{eq}+50$ ns) as a function of equilibration time, t_{eq}. (*Solid line*) Single exponential fit to the mean over $0.5 < t_{eq} \leq 1.5$ μs. (*C*) Mean values of ΔG^0_{bind} from the 10-μs/umbrella simulations (*crosses*) together with the mean values of ΔG^0_{bind} (*triangles*) and exponential fit from panel *B*. PMF and ΔG^0_{bind} profiles obtained from each of the 60 independent simulations are shown in Fig. S1 in the Supporting Material. (*D–F*) Representative conformations after 1.5 μs of simulation at z^0_i = (*D*) 3 nm, (*E*) 1.2 nm, and (*F*) 0.0 nm. To see this figure in color, go online.

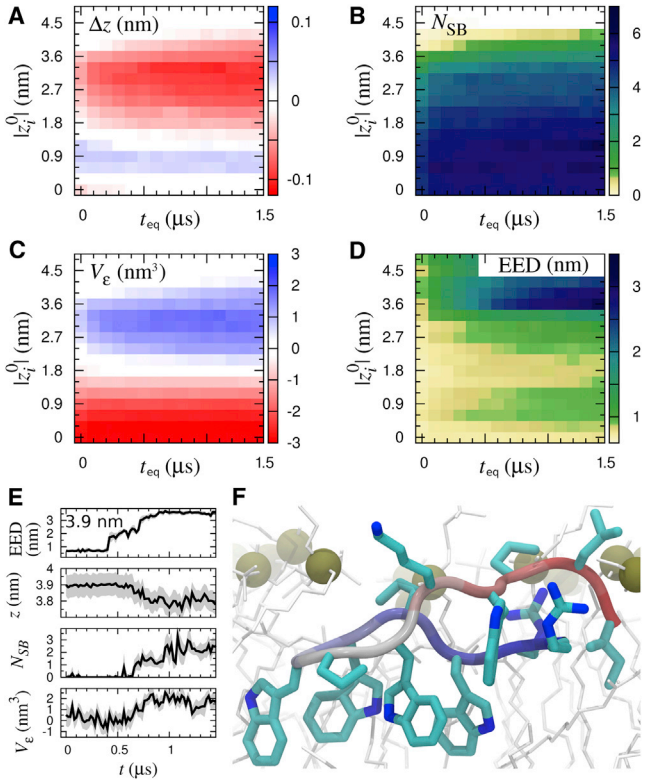

FIGURE 2 Slow equilibration of bilayer and peptide. (*A–D*) Color quantifies conformational reorganization for $t_{eq} < t \leq t_{eq} + 100$ ns as a function of t_{eq} and $|z^0_i|$. (*A*) Deviation of insertion depth, *z*, from z^0_i, $\Delta z \equiv z - z^0_i$; (*B*) number of peptide-lipid salt bridges, N_{SB}; (*C*) volume change of the bilayer's proximal leaflet in the radial vicinity of the solute, V_ϵ; and (*D*) peptide end-to-end distance (EED). There is no sampling for $t > 0.5$ μs at $|z^0_i| \geq 4.5$ nm. (*E*) Representative time-series of a trajectory at $z^0_i = 3.9$ nm. (*F*) Representative conformation at 10 μs for $|z^0_i| = 1.2$ nm. To see this figure in color, go online.

Material). These Boltzmann-weighted ensemble averages may not be mechanistically representative of nonequilibrium binding events (8,10).

The reorganization of the peptide, the bilayer, and the ionic interactions between them became more pronounced with increasing simulation time at peptide insertion depths shallower than the global free energy minimum ($|z^0_i| > 1.4$ nm; Fig. 1 *A* and Fig. 2, *B–D*). These conformational transitions are likely the source of the systematic drift of ΔG^0_{bind}. Reorganization of the bilayer also controls the rate of equilibration during membrane insertion of an arginine side chain (8,9) and a cyclic arginine nonamer (11), suggesting that slow reorganization of lipids around cationic solutes presents a general impediment to simulation convergence.

Consistent with the perturbation of membrane thickness observed by in situ atomic force microscopy (12), our results suggest that indolicidin insertion induces local thinning of the bilayer (Fig. 1, *E* and *F*, and Fig. 2, *C* and *F*). The different conformational ensembles sampled by the peptide in water and in the lipid bilayer (Fig. 2 *D*) are consistent with the observations that indolicidin is disordered in solution (13) and adopts stable conformations in the presence of detergent (14). Although the peptide's conformation continued to change when it was deeply inserted (Fig. 2 *D*), the amount of water in the bilayer's hydrophobic core converged relatively rapidly (see Fig. S2). Indolicidin can induce the formation of hydrated, porelike defects (see Fig. S2, Fig. S3, Fig. S4, and Fig. S5) but does not act as a chloride carrier (see Fig. S6 and Fig. S7). Future studies of the mechanism of indolicidin action will examine the effect of multiple peptide binding.

The PMF profile presented in this Letter is strikingly different from that computed by Yeh et al. (15) using different force field parameters for indolicidin partitioning into a DMPC (1,2-dimyristoyl-*sn*-glycero-3-phosphatidylcholine) bilayer, from which the binding free energy was estimated to be 0 kcal/mol (15). However, that study comprised only 25 ns per umbrella and likely suffers from systematic sampling errors induced by initial conditions (see Fig. S8).

Our estimate of the binding affinity is much larger than the values obtained for indolicidin and large unilamellar POPC vesicles using isothermal titration calorimetry, −7.4 kcal/mol (16), and equilibrium dialysis, −8.8 kcal/mol (13). Such a discrepancy suggests that the relative accuracy of binding free energies for amino-acid side-chain analogs (8,9,17) does not necessarily extend to polypeptides. Although more work is needed to elucidate the source of this discrepancy, this study underlines the importance of attaining convergence before evaluating force-field accuracy.

Importantly, this work also highlights the extensive sampling required to remove systematic errors induced by initial conditions in atomistic simulations of peptides in membranes. Slow equilibration of the system is due to rare transitions across hidden free energy barriers involving reorganization of the membrane. Two simple recommendations are 1), evaluating the time-dependence of ensemble averages, and 2), conducting multiple simulations with different initial conditions. We have recently shown that by using enhanced sampling techniques it is possible to identify the locations of hidden free energy barriers without a priori knowledge (9). Future research will examine strategies for speeding up the crossing of these barriers, such as optimized order parameters including bilayer reorganization and enhanced sampling techniques including a random walk along the order parameter (9).

SUPPORTING MATERIAL

Supplemental Methods and Results, two tables, eight figures, three equations and references (18–24) are available at http://www.biophysj.org/biophysj/supplemental/S0006-3495(14)00275-6.

ACKNOWLEDGMENTS

Computations were performed at SciNet (25) and data was stored at SHARCNET, both of which are resources of Compute Canada.

This work was funded in part by National Sciences and Engineering Research Council discovery grant No. RGPIN-418679 and by Canadian Institutes of Health Research operating grants No. MOP-43998 and No. MOP-43949.

REFERENCES and FOOTNOTES

1. Hancock, R. E. W. 2001. Cationic peptides: effectors in innate immunity and novel antimicrobials. *Lancet Infect. Dis.* 1:156–164.
2. Epand, R. M., and H. J. Vogel. 1999. Diversity of antimicrobial peptides and their mechanisms of action. *Biophys. Biochim. Acta.* 1462: 11–28.
3. Selsted, M. E., M. J. Novotny, …, J. S. Cullor. 1992. Indolicidin, a novel bactericidal tridecapeptide amide from neutrophils. *J. Biol. Chem.* 267:4292–4295.
4. Stein, W. 1986. Transport and Diffusion across Cell Membranes. Academic Press, Orlando, FL.
5. Saiz, L., and M. L. Klein. 2002. Computer simulation studies of model biological membranes. *Acc. Chem. Res.* 35:482–489.
6. Grossfield, A., S. E. Feller, and M. C. Pitman. 2007. Convergence of molecular dynamics simulations of membrane proteins. *Proteins.* 67:31–40.
7. Torrie, G. M., and J. P. Valleau. 1977. Nonphysical sampling distributions in Monte Carlo free-energy estimation: umbrella sampling. *J. Comput. Phys.* 23:187–199.
8. Neale, C., W. F. D. Bennett, …, R. Pomès. 2011. Statistical convergence of equilibrium properties in simulations of molecular solutes embedded in lipid bilayers. *J. Chem. Theory Comput.* 7:4175–4188.
9. Neale, C., C. Madill, …, R. Pomès. 2013. Accelerating convergence in molecular dynamics simulations of solutes in lipid membranes by conducting a random walk along the bilayer normal. *J. Chem. Theory Comput.* 9:3686–3703.
10. Kopelevich, D. I. 2013. One-dimensional potential of mean force underestimates activation barrier for transport across flexible lipid membranes. *J. Chem. Phys.* 139:134906.
11. Huang, K., and A. E. García. 2013. Free energy of translocating an arginine-rich cell-penetrating peptide across a lipid bilayer suggests pore formation. *Biophys. J.* 104:412–420.
12. Shaw, J. E., J.-R. Alattia, …, C. M. Yip. 2006. Mechanisms of antimicrobial peptide action: studies of indolicidin assembly at model membrane interfaces by in situ atomic force microscopy. *J. Struct. Biol.* 154:42–58.
13. Ladokhin, A. S., M. E. Selsted, and S. H. White. 1997. Bilayer interactions of indolicidin, a small antimicrobial peptide rich in tryptophan, proline, and basic amino acids. *Biophys. J.* 72:794–805.
14. Rozek, A., C. L. Friedrich, and R. E. W. Hancock. 2000. Structure of the bovine antimicrobial peptide indolicidin bound to dodecylphosphocholine and sodium dodecyl sulfate micelles. *Biochemistry.* 39:15765–15774.
15. Yeh, I.-C., D. R. Ripoll, and A. Wallqvist. 2012. Free energy difference in indolicidin attraction to eukaryotic and prokaryotic model cell membranes. *J. Phys. Chem. B.* 116:3387–3396.
16. Andrushchenko, V. V., M. H. Aarabi, …, H. J. Vogel. 2008. Thermodynamics of the interactions of tryptophan-rich cathelicidin antimicrobial peptides with model and natural membranes. *Biochim. Biophys. Acta.* 1778:1004–1014.
17. MacCallum, J. L., W. F. D. Bennett, and D. P. Tieleman. 2008. Distribution of amino acids in a lipid bilayer from computer simulations. *Biophys. J.* 94:3393–3404.
18. Hess, B., C. Kutzner, …, E. Lindahl. 2008. GROMACS 4: algorithms for highly efficient, load-balanced, and scalable molecular simulation. *J. Chem. Theory Comput.* 4:435–447.
19. Jorgensen, W. L., J. Chandrasekhar, …, M. L. Klein. 1983. Comparison of simple potential functions for simulating liquid water. *J. Chem. Phys.* 79:926–935.
20. Berger, O., O. Edholm, and F. Jähnig. 1997. Molecular dynamics simulations of a fluid bilayer of dipalmitoylphosphatidylcholine at full hydration, constant pressure, and constant temperature. *Biophys. J.* 72:2002–2013.
21. Kaminski, G. A., R. A. Friesner, …, W. L. Jorgensen. 2001. Evaluation and reparametrization of the OPLS-AA force field for proteins via comparison with accurate quantum chemical calculations on peptides. *J. Phys. Chem. B.* 105:6474–6487.
22. Kandt, C., W. L. Ash, and D. P. Tieleman. 2007. Setting up and running molecular dynamics simulations of membrane proteins. *Methods.* 41: 475–488.
23. Ferrenberg, A. M., and R. H. Swendsen. 1988. New Monte Carlo technique for studying phase transitions. *Phys. Rev. Lett.* 61:2635–2638.
24. Rokitskaya, T. I., N. I. Kolodkin, …, Y. N. Antonenko. 2011. Indolicidin action on membrane permeability: carrier mechanism versus pore formation. *Biochim. Biophys. Acta.* 1808:91–97.
25. Loken, C., D. Gruner, …, R. Van Zon. 2010. SciNet: lessons learned from building a power-efficient top-20 system and data centre. *J. Phys. Conf. Ser.* 256:012026.